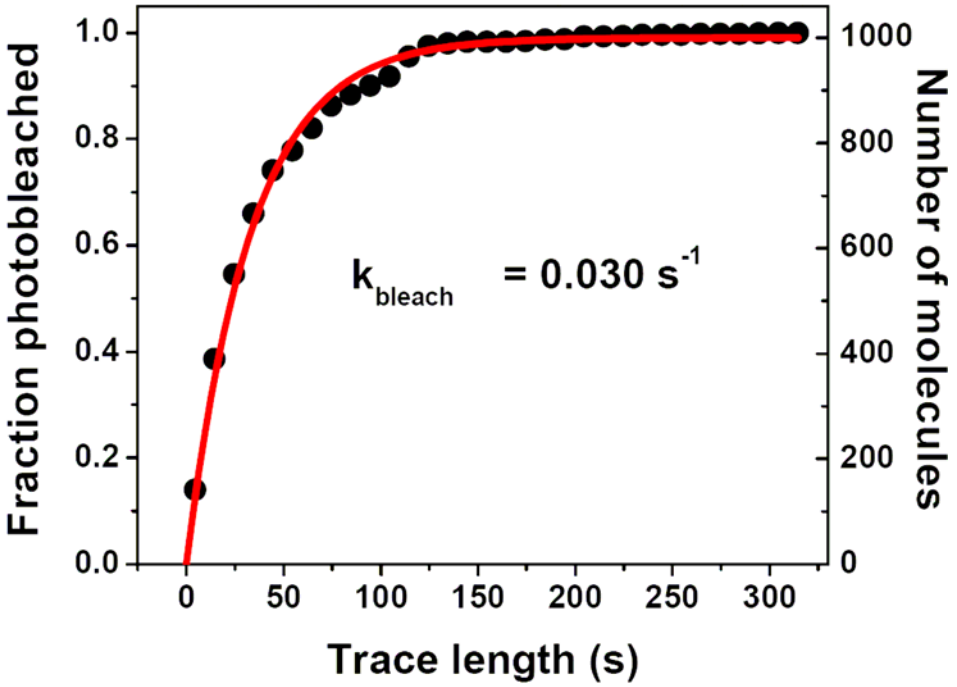

Figure S1: Histogram of the lengths of FRET traces. The line shows the best single-exponential fit, from which the rate constant k_{bleach} was determined.

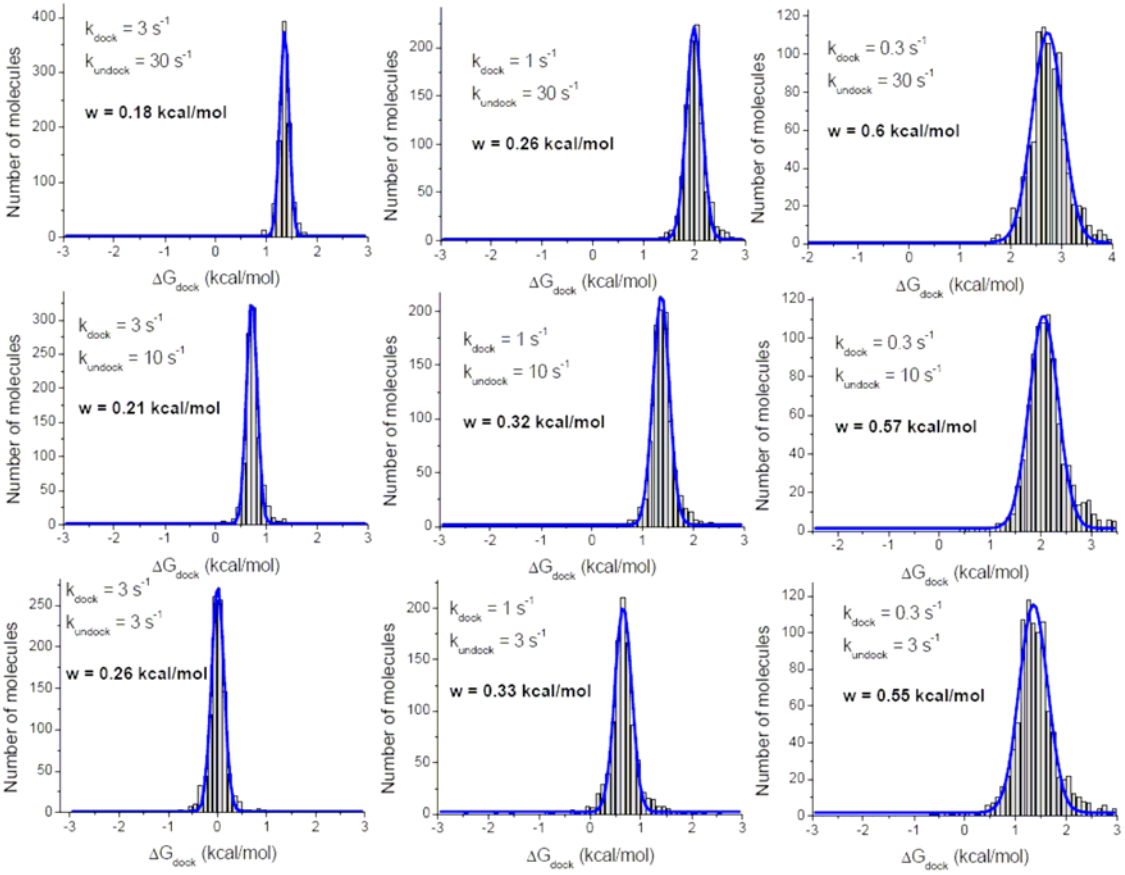

Figure S2: Simulated distributions of ΔG_{dock} for two-state FRET fluctuations with varying k_{dock} and k_{undock}. Each distribution was simulated for 1000 FRET traces, "photobleaching" with a rate constant $k_{bleach} = 0.03\ s^{-1}$. The input values of k_{dock} and k_{undock}, and the width ($w = 2\sigma$) obtained from a Gaussian fit are indicated on the plots.

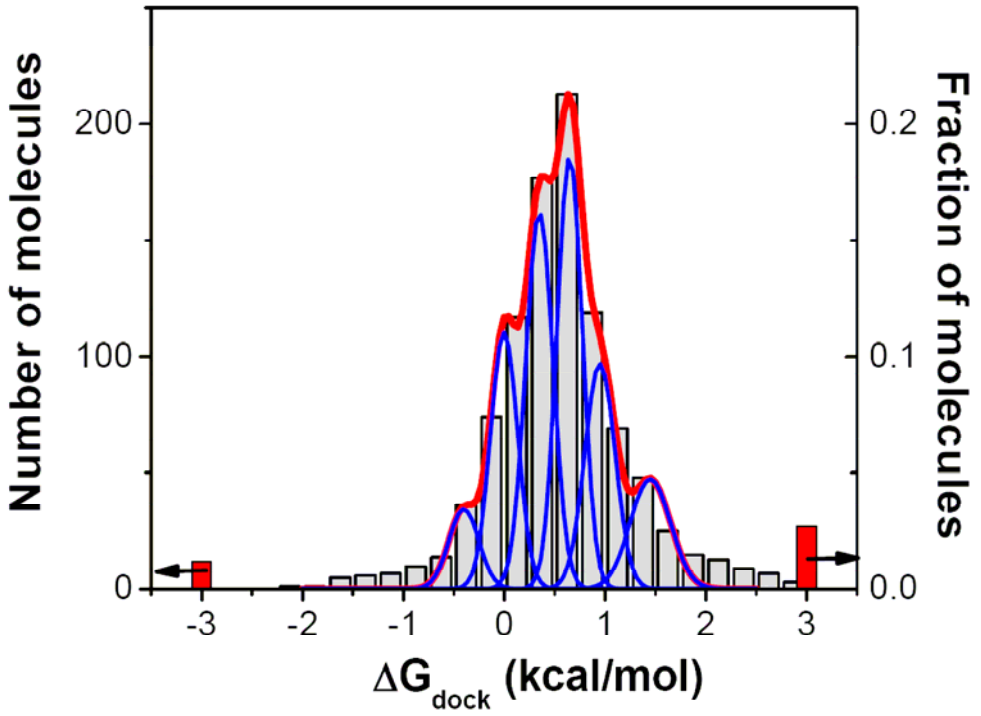

Figure S3: Fit of the experimentally observed ΔG_{dock} distribution with a sum of six conformations. Because of complexity of fitting with 18 free parameters, for each of the conformations ΔG_{dock} was manually chosen, width (w) was fixed to a value determined from the simulations for the corresponding ΔG_{dock} (k_{dock} and k_{undock} for each ΔG_{dock} were taken from the distribution in Fig. 1f), and only the amplitudes allowed to freely float.

Comparing the widths of ΔG_{dock} distributions for different oligonucleotide substrates.

Our data indicate that there are several active conformations of the ribozyme, at least six and likely considerably more. We assayed the origins of the conformational heterogeneity by probing the ability of the ribozyme to make specific interactions with the P1 duplex. If a subset of the ribozyme conformations misaligned a structural element responsible for a specific tertiary interaction with the P1 duplex, then removal of the P1 functional group making that interaction would have no effect on docking of those molecules, while RNAs that did make this interaction would have destabilized docking. Such a shift for only a subset of the RNAs would collapse or narrow the distribution of docking behaviors. We have seen precisely this behavior, using P1 duplex with a methoxy group substituting for a 2'-hydroxyl group that makes an important tertiary interaction in docking (Fig. S4). Docking free energy distributions were obtained for two substrates (-1d)S and (-3m)S, as described above. Measurements for both substrates were performed under identical conditions using the same ribozyme sample. The width of each distribution was measured by fitting the whole distribution to a single Gaussian and taking the standard deviation parameter of the best fit. The width of the distribution for (-3m)S is significantly smaller than for the (-1d)S, consistent with the model that the 2'-hydroxyl group in (-3) position makes tertiary docking interactions in only a sub-set of the ribozyme conformers.

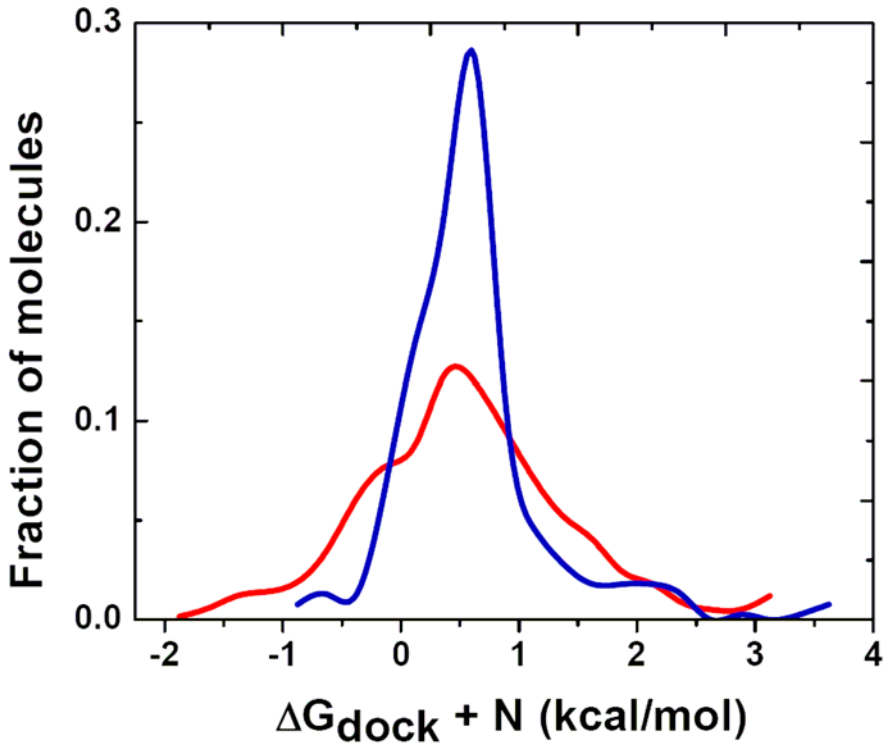

Figure S4: Comparison of ΔG_{dock} distributions for (-1d)S (red line) and (-3m)S (blue line) substrates. The widths of the distributions is 1.5 and 0.7 kcal/mol, respectively. The ΔG_{dock} distribution for (-1d)S was uniformly shifted by N = +1.5 kcal/mol to overlay it with the distribution for (-3m)S for easier visual comparison. The actual midpoints of the distributions were X and Y for (-1d)S and (-3m)S were –1.0 and 0.5 kcal/mol, respectively.

Comparing widths of ΔG_{dock} distributions with different immobilization strategies.

To test if the broadened distribution is caused by interactions of the tethered of molecules with the BSA-covered quartz surface, we measured docking using a different surface and alternative strategy that immobilizes molecules inside lipid vesicles, as suggested by Okumus et al.[1] Briefly, 1 mg of lipid (99% egg lecitin, 1% cap-biotin PE) chlorophorm solution was dried into a thin film and re-dispersed by vortexing with 0.2 ml of the standard buffer containing 100 nM pre-formed ternary complexes L-16T2/T2-Cy5/S-Cy3 (non-biotinylated DNA tether was used for these experiments). Vesicles were prepared by ~20 rounds of extrusion of the mixture through a 100 nm pore size filter and used within 6 hours. Quartz slides were coated with biotinylated lipids by incubating them with the suspension of empty vesicles (prepared as above, but omitting ternary complexes from the buffer) for 1 hour. Slides were then washed and covered with streptavidin as described above. Vesicle-encapsulated ternary complexes were bound to the surface at 1:50 dilution (final concentrations 0.1 mg/ml of lipids, 2 nM of ternary complexes) and non-tethered vesicles and non-encapsulated complexes were removed by extensive washing with the standard buffer. Control experiments indicated that non-specific binding of complexes to lipid-coated surfaces is low (less than one molecule per field of view is detected for non-vesicle-encapsulated complexes; data not shown). Data acquisition and analysis were preformed exactly as described above for molecules tethered to BSA-covered slides.

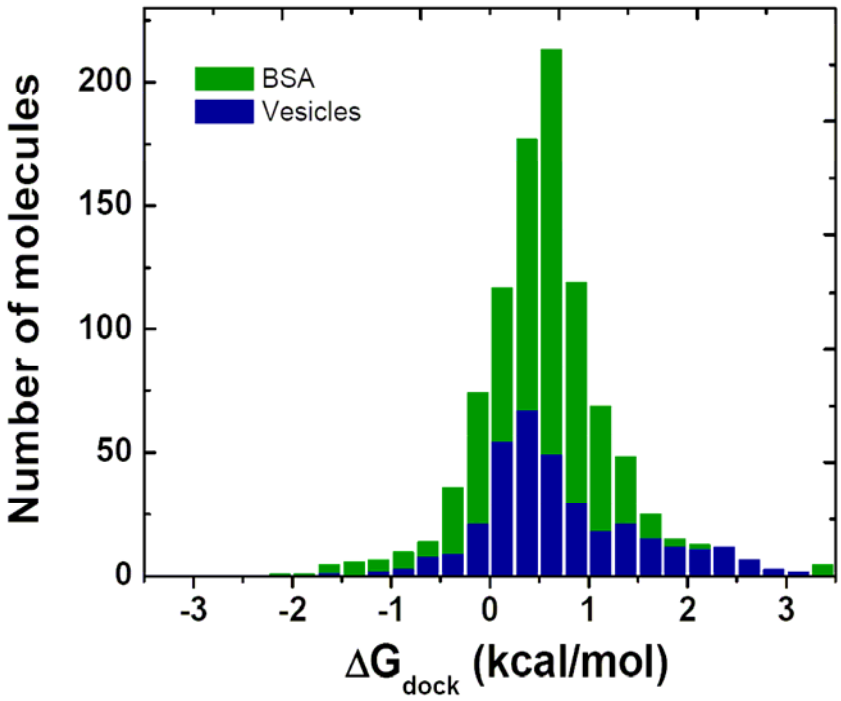

Figure S5: Comparison of ΔG_{dock} distributions for BSA surface-tethered molecules (green) and lipid vesicle-encapsulated molecules (blue). The widths of the distributions are 0.92 and 0.91 kcal/mol, respectively.

Disappearance of substrate fluorescence corresponds to substrate cleavage.

The activity of the ribozyme was measured as the rate of disappearance of substrate fluorescence. Multiple other processes, such as photobleaching, substrate dissociation, or dissociation of molecules from the surface can contribute to the observed rate constant. Control experiments establishing the total contribution of these processes to the observed rate constants were performed, in which the rate of substrate fluorescence disappearance was measured in the absence of guanosine. As is shown in Fig. S6, disappearance of the fluorescence spots in the presence of guanosine is much faster than in the control experiment. Photobleaching is likely to be the dominant reason for the disappearance of spots in the conditions of the control experiment. The rate of substrate dissociation and guanosine-independent cleavage might also contribute to the observed rate constant.

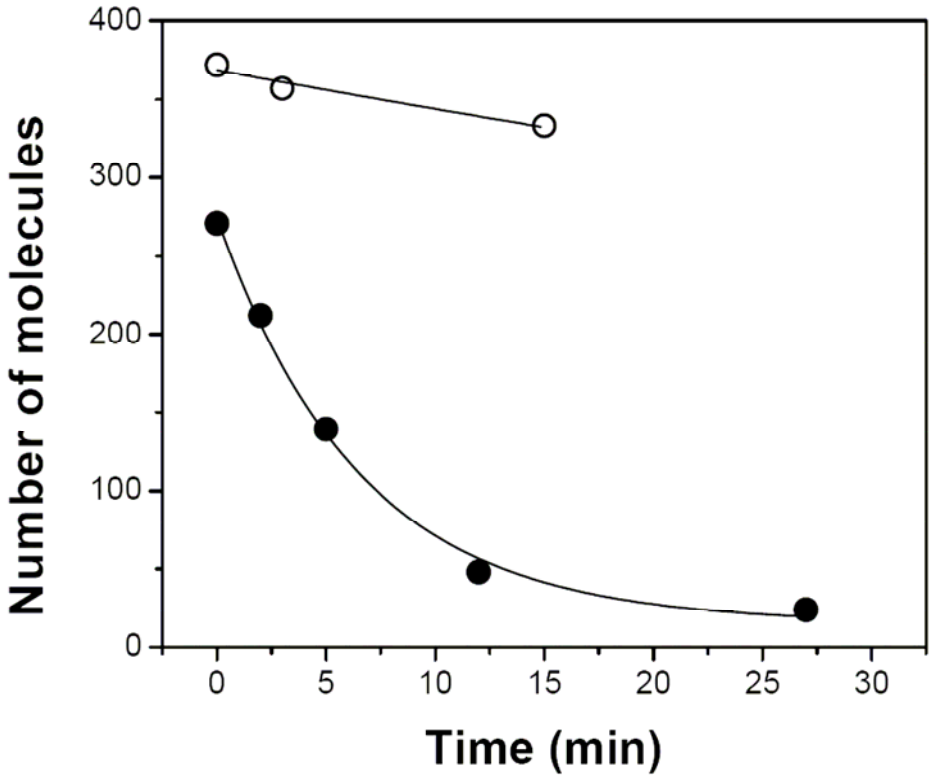

Figure S6: Disappearance of fluorescent spots is much slower in the absence of guanosine (open circles, line shows the best fit to a single-exponential decay, k_{off} = 0.007

min^{-1}), than in the presence of guanosine (filled circles, line shows the best fit to a single-exponential decay, k_{off} = 0.16 min^{-1}).

Comparing cleavage kinetics for ribozyme molecules exhibiting different docking behaviors.

Table 1: **Kinetic parameters for molecules from different bins are the same**†

Bin	I (red)	II (green)	III (blue)	IV (violet)	V (black)	Global (line)
Number of molecules	61	146	196	107	31	541
k_{cleav} (min^{-1})	0.14 ± 0.02	0.16 ± 0.02	0.16 ± 0.03	0.13 ± 0.02	0.18 ± 0.08	0.16 ± 0.08
Endpoint (%)	9 ± 3	1 ± 7	6 ± 10	1 ± 4	20 ± 5	6 ± 3

† Bins are identified according to the colors in Fig. 3a in the main text. The range of ΔG_{dock} from bin I to bin V was >4 kcal/mol, corresponding to >800-fold difference in K_{dock}. Errors represent s.e.m from fitting.

The difference in K_{dock} between bins I-IV was not expected to result in measurable differences in catalytic activity, because in each of these bins the substrate is docked at least 60% of the time. In bin V the substrate is, on average, 20% docked, which is mostly simply expected to result in ~5-fold lower activity. The most likely reason for not observing lower activity for these molecules is the thermodynamic coupling between guanosine binding and substrate docking.[2] Approximately 10-fold cooperativity should cause the substrate to be at least 60% docked with guanosine bound even for the molecules that have the substrate only 20% docked without guanosine bound.

The same average catalytic activity for different bins does not mean that all individual molecules have the same catalytic activity, because we observed only one turnover for each molecule, and determined k_{cleav} by binning together multiple molecules. Individual molecules can have different levels of activity, but as long as there are approximately equal numbers of molecules with each activity level among different docking bins, all bins would have the same average activity.

Unfolding/refolding experiments

Forty percent of the total number of molecules did not display any docking transitions after refolding (the rightmost bin marked by an arrow in Fig. 4c). These molecules likely folded to a long-lived "misfolded" state described in previous studies.[3,4] A somewhat lower fraction of molecules misfolding in our experiments (40% *vs.* 80% in previous studies) may indicate incomplete equilibration between unfolded conformations that tend to fold correctly or to misfold. Approximately half of these molecules started docking after unfolding-refolding cycle was repeated (*data not shown*), consistent with population of a misfolded state as opposed to loss of the acceptor dye to photobleaching. These misfolded molecules are practically absent in the original distribution because pre-folding conditions (50 ^{o}C) ensure that misfolded ribozyme fully converts into the active form.[3]

To demonstrate that molecules across the distribution changed their behavior, three groups of molecules were selected from the distribution before unfolding, as shown by red, blue and green bars in Fig. 4b. To make sure that these groups do not overlap and molecules from one group are not misidentified as belonging to another group, two bins on both sides of the middle, "blue", group were excluded from the analysis (clear bars). The probability of misidentifying a "blue" molecule as a "red" or a "green" was 1.0%, the probability of misidentifying a "red" molecule as a "blue", or a "green" as a "blue", was approximately 0.6%.

Docking behavior of the molecules from the "red", "blue" and "green" groups after refolding is indicated by the corresponding colors in the distribution in Fig. 4c. The height of the colored bars represents the number of molecules from the three groups

within each bin. Overlap between these distributions indicates that molecules change their behavior during refolding. The probabilities that any of the molecules from the three groups would be observed in the bins more than one bin away from their original position without changing docking behavior were estimated from the simulations to be ~ 0.1%. This probability corresponds to observing 0.3 molecules moving by more than one bin, while ~ 30 such molecules were actually observed, which is significantly larger ($P<10^{-16}$) assuming Poisson statistics for the number of observed molecules.

To test whether molecules interconvert in the folded state, the experiment and analysis were performed as described above, except unfolding by EDTA was omitted. Fig. 4d shows the extent of interconversion 40 min after the initial distribution of the molecules was observed. The “red”, the “blue” and the “green” distributions largely remained centered at their original positions. There was also relatively little overlap between distributions, with most molecules moving only to the next bin. Only a small fraction of molecules from each bin moved by more than one bin during the 40 min time period.

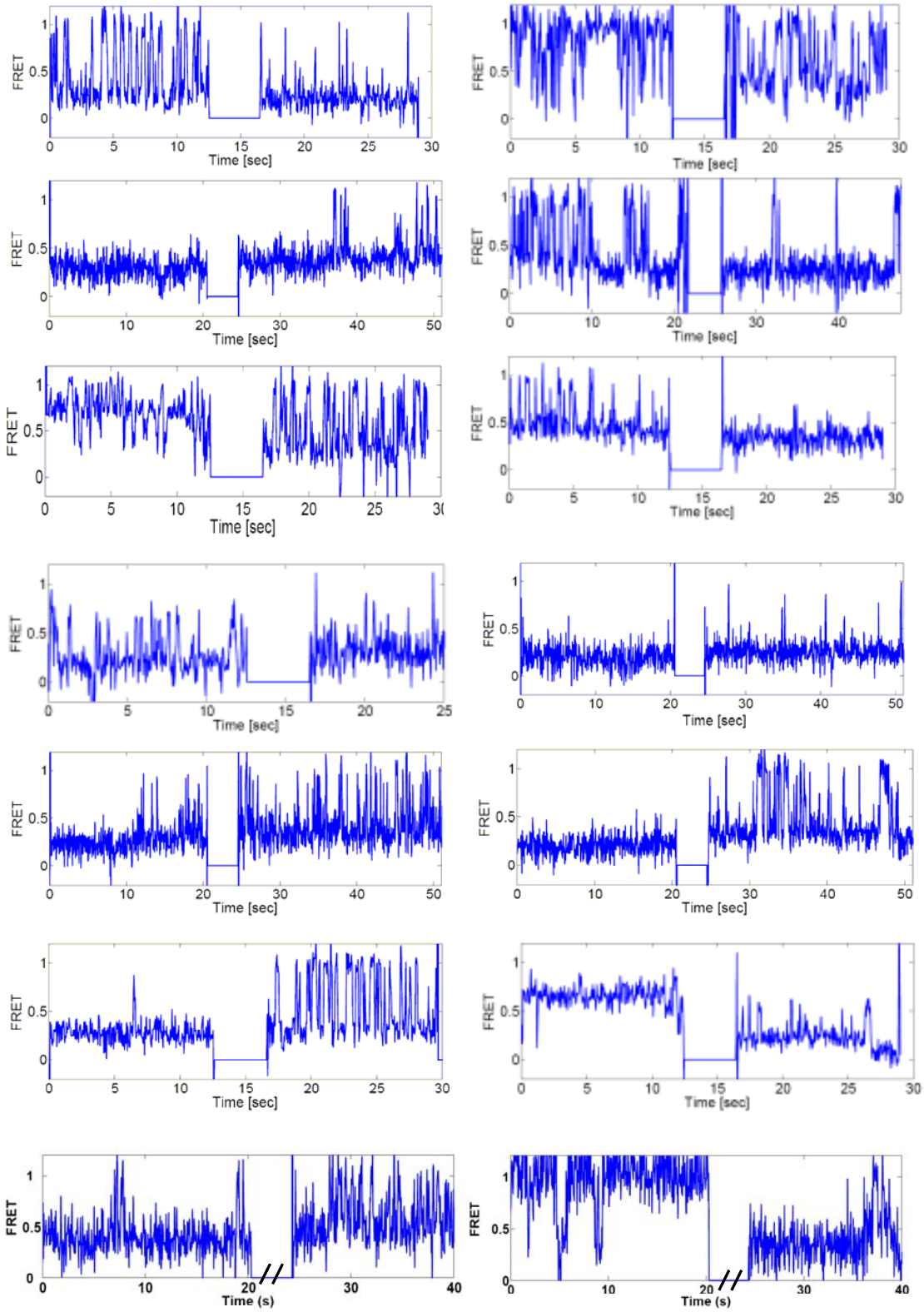

Figure S7: Additional examples of FRET traces showing exchange of docking behaviors.

References:

1 Okumus, B., Wilson, T.J., Lilley, D.M.J., and Ha, T. Vesicle Encapsulation Studies Reveal that Single Molecule Ribozyme Heterogeneities Are Intrinsic. *Biophys. J.* **87**, 2798 (2004).

2 Karbstein, K., Lee, J., and Herschlag, D. Probing the Role of a Secondary Structure Element at the 5' and 3'-Splice Sites in Group I Intron Self-Splicing:The Tetrahymena L-16 ScaI Ribozyme Reveals a New Role of the G-U Pair in Self-Splicing. *Biochemistry* **46**, 4861 (2007).

3 Russell, R. and Herschlag, D. Probing the folding landscape of the Tetrahymena ribozyme: commitment to form the native conformation is late in the folding pathway. *J. Mol. Biol.* **308**, 839 (2001).

4 Russell, R. et al. Exploring the folding landscape of a structured RNA. *Proc. Natl. Acad. Sci. U. S. A.* **99**, 155 (2002).